

Review

# Blazar Optical Polarimetry: Current Progress in Observations and Theories

Haocheng Zhang 

Department of Physics and Astronomy, Purdue University, West Lafayette, IN 47907, USA;  
astrophyszhc@hotmail.com

Received: 2 September 2019; Accepted: 22 October 2019; Published: 27 October 2019



**Abstract:** Polarimetry has been a standard tool to probe the active galactic nucleus (AGN) jet magnetic field. In recent years, several optical polarization monitoring programs have been carried out, bringing in many exciting new results and insights into jet dynamics and emission. This article discusses current progress in blazar optical polarimetry. The main focus is the variability of polarization signatures, which has spurred a lot of theoretical studies. These novel developments have provided unique constraints on the blazar flares and emphasized the role of the magnetic field in jet evolution. Optical polarimetry will continue to act as an essential component in the multi-messenger study of AGN jets, in particular with the upcoming high-energy polarimetry. Comparing to first-principle numerical simulations, future multi-wavelength polarimetry can shed light on jet dynamics, particle acceleration, and radiation processes.

**Keywords:** active galaxies; blazars; polarization

## 1. Introduction

Relativistic jets from active galactic nuclei (AGNs) are powered by strong accretion onto central supermassive black holes. These plasma jets can stay highly collimated during their propagation through space, extending to kilo-parsec (kpc) or even up to mega-parsec (Mpc) scales (see, e.g., [1,2]). They are the most powerful astrophysical systems in our universe, showing bright emission from radio up to TeV  $\gamma$ -rays (e.g., [3–6]). Jet emission is non-thermal-dominated and highly variable. Blazars are a subclass of AGNs whose jets point very close to our line of sight. Due to relativistic beaming, their apparent luminosity is strongly boosted, making them the most numerous extragalactic  $\gamma$ -ray sources [7,8]. Blazars consist of flat spectrum radio quasars (FSRQs) and BL Lac objects (BL Lacs). The difference is that BLLacs generally do not show strong emission lines in the optical band. For recent reviews on blazars, see, for example, [9,10].

Blazars exhibit a broadband nonthermal spectrum extending from radio to  $\gamma$ -rays. This spectrum consists of a low-energy component and a high-energy component. The low-energy component usually goes from radio to infrared/optical, and in some cases it can extend to soft X-rays. The high-energy component extends from X-rays to  $\gamma$ -rays. The low-energy component is dominated by the synchrotron emission of relativistic electrons. This is evident by the high linear polarization degree in the radio to optical bands (e.g., [11,12]). The high-energy component may be explained by either leptonic or hadronic scenarios. The leptonic scenario assumes that the same electrons that make the low-energy synchrotron component can inverse Compton scatter low-energy photons to high energies. The source of the low-energy photons can come from either the synchrotron emission itself (synchrotron-self Compton, SSC, [13,14]) or external sources such as the thermal emission from the broad line region and dusty torus (external Compton, EC, [15–17]). Spectral fitting with leptonic models usually assumes a relatively low magnetic field, typically from mG to G levels [18,19]. On the other hand, the hadronic models suggest that the protons may be accelerated to very high energies, then produce the high-energy

component via proton synchrotron and/or photomeson processes [20–22]. Depending on the model parameters, the SSC from electrons can contribute to the high-energy component in the hadronic model as well [18]. Hadronic models generally predict the production of neutrinos in jets. In the case of proton synchrotron models, the required magnetic field is usually strong ( $\gtrsim 10$  G), and the acceleration of ultra high energy cosmic rays (UHECRs) in the blazar jet is often necessary [18,23]. Both scenarios can reproduce the typical blazar spectra and light curves (see, e.g., [24–28]). Recently, the IceCube-170922A event showed the first potential association of a very high energy neutrino detection with the flaring blazar TXS 0506+056, opening a multi-messenger window for the study of AGN jets, and IceCube has discovered 13 neutrino events from the same direction in the 2014–2015 period [29,30]. Nonetheless, so far, theoretical studies find it very controversial how the blazar jets accelerate protons to very high energy and produce the neutrino and blazar flare events (refer to, e.g., [31–35]).

Clearly, additional information beyond spectra and light curves are necessary to better understand jet physics. Polarization signatures can probe the magnetic field structure and evolution in AGN jets. Radio and optical polarimetry have been successfully run for decades, providing direct constraints on the jet magnetic field (e.g., [36–39]). Recent optical polarization monitoring programs have made significant efforts in collecting both spectral and temporal optical polarization data. These observations have shown that polarization signatures can be highly variable, especially during blazar flaring activities [40–43]. Very interestingly, optical polarization angle swings have been reported in correlation with multi-wavelength flares, indicating active magnetic field evolution during flares [44–46]. These results are consistent with predictions of recent first-principle numerical simulations, which have also demonstrated that the magnetic field in jets can play a crucial role in jet dynamics and particle acceleration (e.g., [47–50]). Furthermore, predictions on multi-wavelength polarimetry have suggested that future X-ray and  $\gamma$ -ray polarimetry alongside optical polarimetry can be powerful diagnostics of proton acceleration and neutrino emission in AGN jets [51,52].

This article reviews recent progress in the optical polarimetry of blazar jets. Section 2 covers results from the optical polarization monitoring programs, focusing on the time-dependent signatures. Section 3 summarizes current theoretical interpretations of these phenomena, especially the polarization angle swings. Section 4 discusses future prospects of optical polarimetry in the multi-messenger era. Although the goal of this article is to provide a balanced overview of optical polarimetry studies, it may be biased by the relevance to the above topics and the author's research interests.

## 2. Progress in Observations

Blazar optical emission can be linearly polarized up to  $\sim 50\%$  [11,53,54]. Circular polarization is hardly detected in blazars (but see [55] for potential detection in quasars). Therefore, the term polarization usually refers to linear polarization in the optical bands. Both polarization degree and angle are commonly reported in the literature. In some cases, the polarized flux, a part of total flux that is equivalent to 100% linear polarization, is reported along with the polarization degree [56]. This number can help to identify whether there is a newly emerging polarized/unpolarized emission component in the jet. In this section, we highlight some recent discoveries in the optical polarization measurement of blazar jets, with an emphasis on the very interesting polarization angle rotations.

### 2.1. Overview

Since the launch of the Fermi  $\gamma$ -ray telescope, the optical spectropolarimetric measurements of blazars have been performed by several programs, such as the Steward Observatory blazar monitoring program<sup>1</sup> and the Boston University blazar program,<sup>2</sup> as a complement to the multi-wavelength

---

<sup>1</sup> <http://james.as.arizona.edu/~psmith/Fermi/DATA/data.html>.

<sup>2</sup> <http://www.bu.edu/blazars/mobpol/mobpol.html>.

spectra and light curves [40,46,57–60]. The optical polarization signatures can be different from the radio counterparts because the radio emission usually comes from a much larger portion of the jet. The optical polarization degree is typically at  $\sim 10\%$ , but sometimes it can reach significantly higher values, especially during flares [45,53,61]. The polarization angle apparently does not always align with the radio jet direction (e.g., [62,63]). The polarization signatures between different optical bands are generally consistent.

Long-term optical polarization monitoring reveals that the overall temporal polarization signatures appear erratic ([57,58,64,65], and see Figure 1 for examples). However, particularly during active states, both the polarization degree and angle can exhibit systematic changes, with reported variability time scales ranging from months down to hours [57,65–67]. Several patterns are frequently reported in the literature. One is that the polarization degree can increase during the flare [56,68,69]. This may originate from a shock that compresses the initially turbulent magnetic field [70] or the emergence of a new, strongly polarized emission zone [56]. In some cases, the polarization signatures are very erratic during flares, which may be attributed to the turbulent magnetic field structure [71]. A rare but very interesting behavior is the polarization angle rotation. These rotations generally happen together with blazar flares [44,72,73], indicating considerable change in the jet structure and/or the magnetic field morphology.

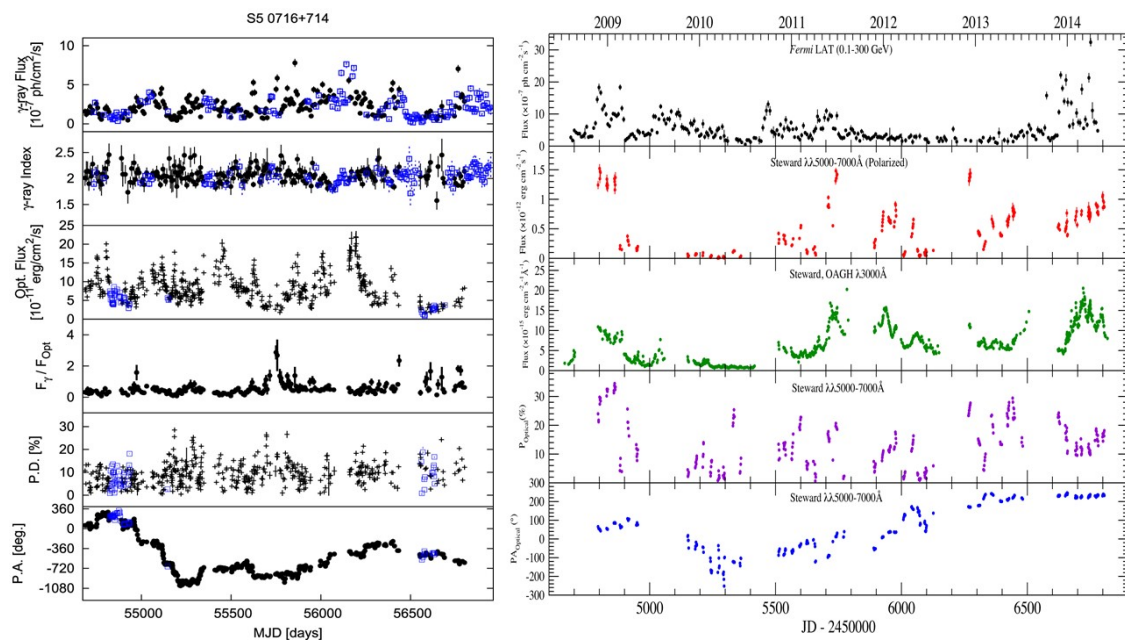


**Figure 1.** Two examples of long-term optical and  $\gamma$ -ray monitoring with optical polarization signatures. **(Left):** Observations of the blazar S5 0716+71 from 2008–2014. The top panel shows the gamma-ray light curve, the second panel shows variability of the gamma-ray spectral index, the third panel shows the optical V-band light curve, the fourth panel shows the ratio of gamma-ray to optical flux, the fifth panel shows variability of the polarization degree, and the bottom panel shows variability of the polarization angle. The figure is reproduced from Figure 1 in [58] with the permission of the American Astronomical Society (AAS). **(Right):** Observations of the blazar 3C 279 from 2008–2014. The temporal behaviors of the polarimetric observations (P, PA, polarized flux) compared with the gamma-rays and the UV-continuum for 3C 279. The figure is reproduced from Figure 4 in [64].

The RoboPol<sup>3</sup> program makes the first attempt to study the statistical patterns of optical polarization signatures (see Figure 2 for some trends that they have found). They have gathered

<sup>3</sup> <http://robopol.org/>.

several years of polarization measurements for tens of  $\gamma$ -ray-loud and  $\gamma$ -ray-quiet blazars, with no preference for whether or not the target blazar is in active state, so as to perform a systematic study of the polarization variability. Based on their sample,

- The average polarization degree of  $\gamma$ -ray-loud blazars appears systematically higher than  $\gamma$ -ray-quiet ones [74].
- The overall polarization temporal behaviors are similar regardless of whether the blazar is detected in the TeV band [75].
- The average polarization degree seems to decrease with a higher peak location of the synchrotron spectral component [74] (this trend has been found in previous works [76,77]).
- The polarization degree variability cannot be completely reproduced by random walk simulations [78].

These trends hint at the potential connection of the overall polarization signatures to the “blazar sequence” [79]. Additional observational data can examine the robustness of these trends, and if confirmed, what the physical causes are.

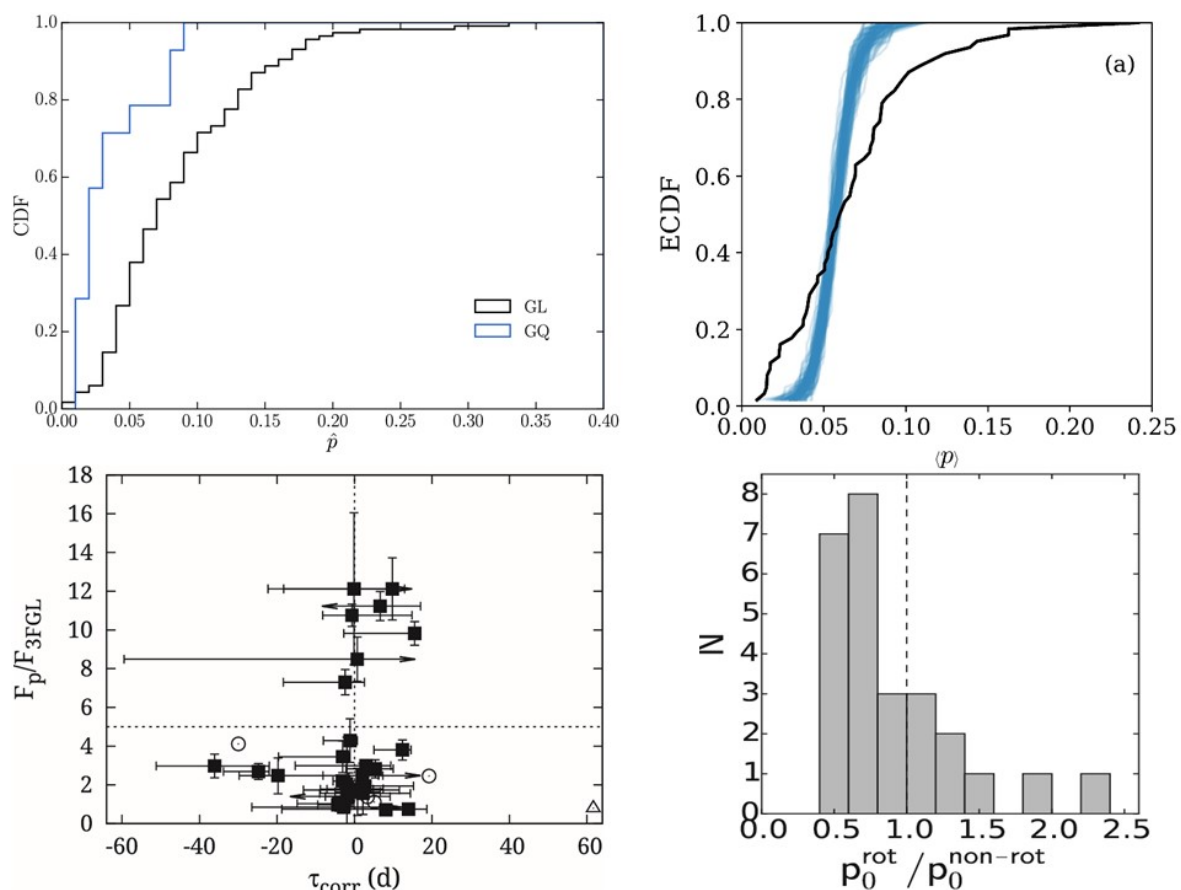


**Figure 2.** Statistical studies of the RoboPol data. (**Upper left**): gamma-ray-loud (GL) blazars show a systematically higher polarization degree than the gamma-ray-quiet (GQ) ones. The figure is reproduced from Figure 1 in [74]. (**Upper right**): observed polarization degree distribution (black line) versus random walk simulations (blue lines). Figure reproduced from Figure 15 in [78]. (**Lower left**): normalized gamma-ray flare level versus time lag between gamma-ray flare and polarization angle rotation. Figure reproduced from Figure 5 in [73]. (**Lower right**): the distribution of the ratio of polarization degree during angle rotation over that outside the angle rotation. Figure reproduced from Figure 9 in [80].

## 2.2. Polarization Angle Rotation

The polarization angle usually shows small erratic fluctuations. Sometimes it can continuously rotate in one direction, and in very rare cases, it can swing  $\sim 180^\circ$  or even beyond that. Such events were first discovered simultaneously with multi-wavelength blazar flares in ([44,81], see Figure 3), indicating major changes in the magnetic field during flares. Notice that [81] does not include Steward Observatory data in the analysis. By including those data, the polarization angle swing is not present. Since the polarization angle has the  $180^\circ$  ambiguity, it requires close sampling of data points to establish a polarization angle swing. Recent optical polarization monitoring programs have collected a large number of polarization angle data and demonstrated that such swings can be present in a number of blazars (see, e.g., [46,58,65,75]).

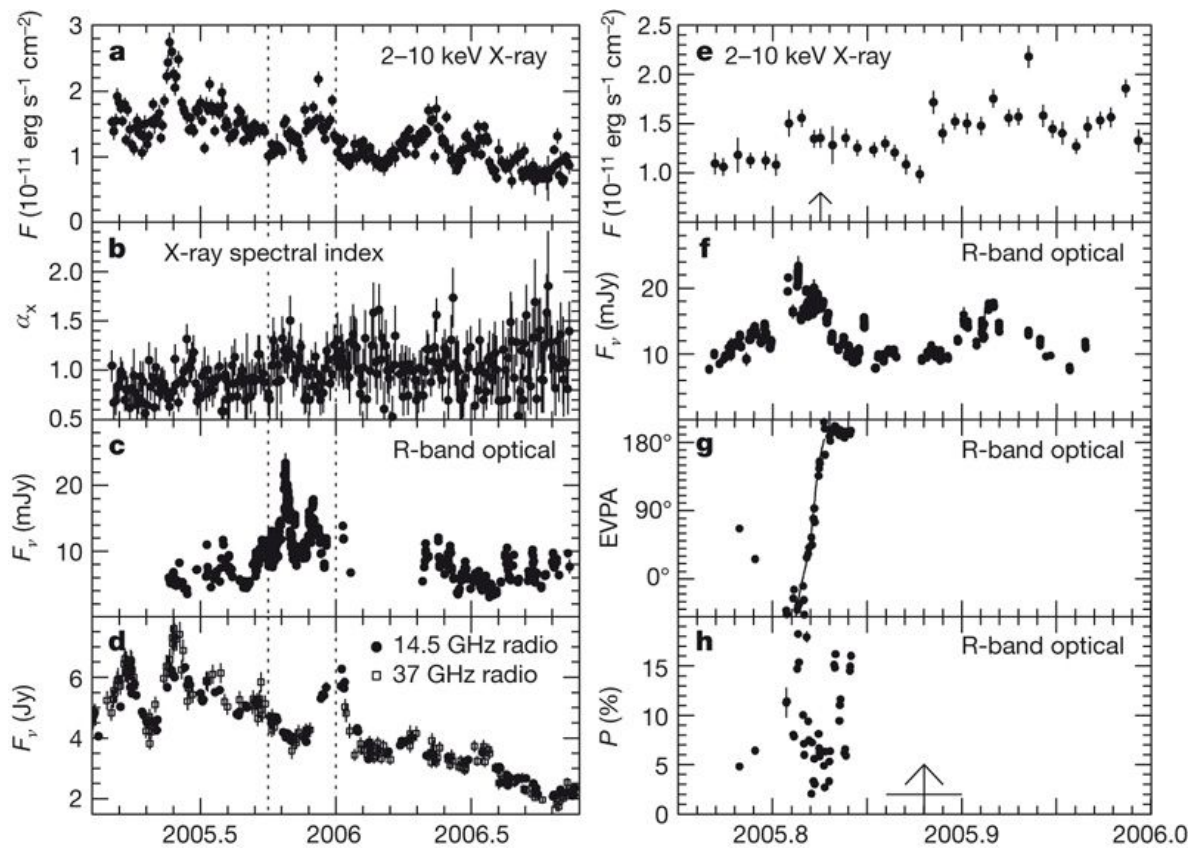


**Figure 3.** Observations of BL Lac showing multi-wavelength flares with an optical polarization angle swing. (a–d), dependence on time of the flux of radiation from BL Lac over a two-year interval at the indicated wavebands. (e–h), enlargements of the 0.25 yr time interval marked by vertical dotted lines in panels (a–d) but with optical R-band polarization angle (g) and degree of polarization P (h) respectively replacing the X-ray spectral index (b) and radio flux density (d) (whereas e and f, respectively, show the magnified intervals in (a,c)). The figure is reproduced from Figure 2 in [44] with permission from Nature.

Although large polarization angle rotations ( $\gtrsim 90^\circ$  rotation) are very rare events, they have been reported in both FSRQs and BL Lacs [80]. Here we highlight some interesting features in the observations (see Figure 4 for some examples). Many large polarization angle swings rotate  $\sim 180^\circ$  [46,74]. So far, the largest polarization angle swing is  $\sim 720^\circ$  [57]. Almost all of these large rotations are reported to be simultaneous with multi-wavelength blazar flares [73]. Given the limited samples, this may be a selection bias, since optical polarimetry is often performed when there are flaring activities (but see RoboPol data for unbiased observations). In most cases, the polarization degree is strongly varying along with the swings [45,57]. The timescale of these angle swings are

typically in days to weeks [46,57,58]. With the increasing reports of polarization angle swings, it is now recognized that these swings can happen in either direction in the same source [53,72].

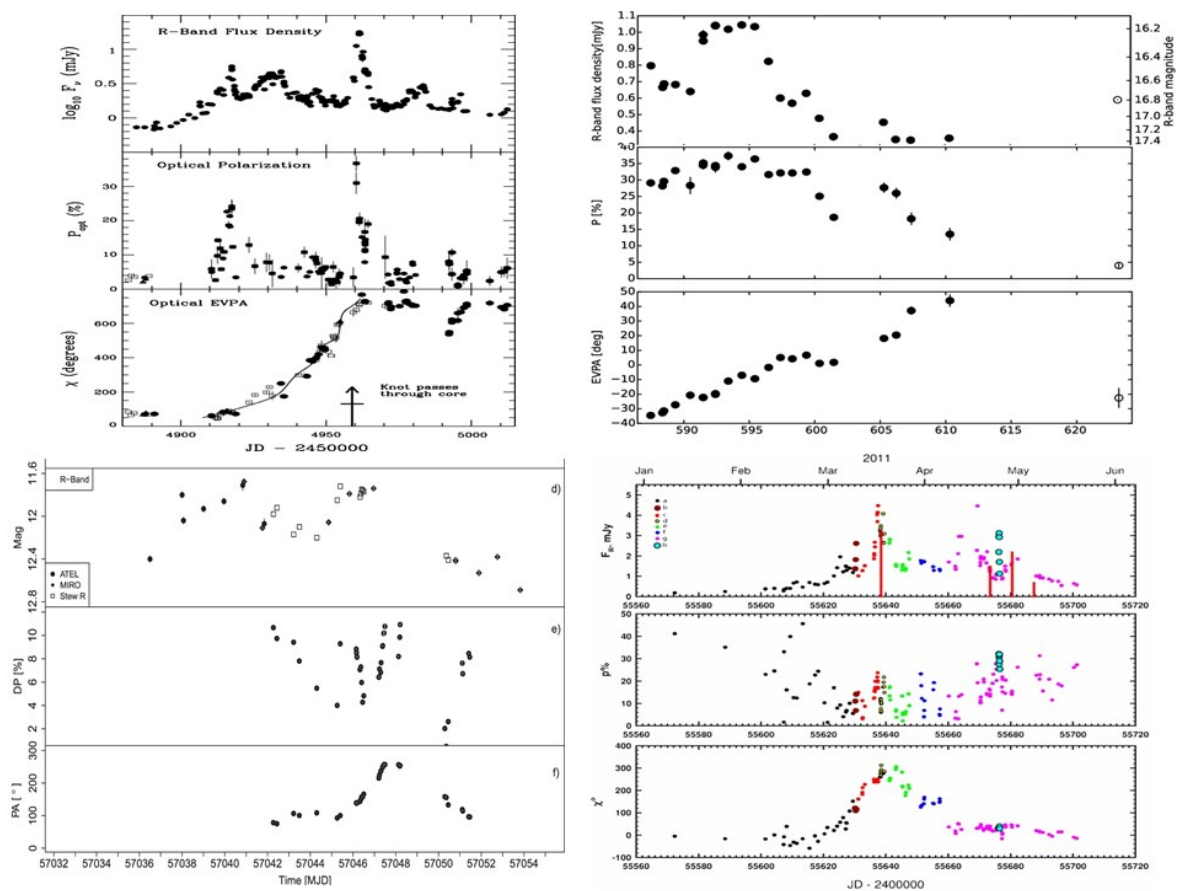


**Figure 4.** Examples of optical polarization angle rotations. All four observations, from top to bottom, show the optical flux, polarization degree, and polarization angle. Upper left: PKS 1510+089. This figure is reproduced from Figure 4 in [57], with permission from the American Astronomical Society (AAS). Upper right: B2 2308+34. This figure is reproduced from Figure 2 in [46]. Lower left: S5 0716+71. This figure is reproduced from Figure 1 in [72], with permission from the American Astronomical Society (AAS). Lower right: S4 0954+658. This figure is reproduced from Figure 2 in [53], with permission from the American Astronomical Society (AAS).

The RoboPol program has significantly boosted the number of observed polarization angle swings. They have attempted statistical study based on their data sample, in which they have found several interesting trends:

- Polarization angle swings are associated with  $\gamma$ -ray flares, with little time lag [73].
- Polarization angle swings do not happen in all blazars, but they can happen in both FSRQs and BL Lacs [80].
- Blazars that have shown rotations generally have brighter and more variable  $\gamma$ -ray emission [80].
- The polarization degree generally decreases during angle rotations [80].
- It is unlikely that all rotations are consistent with random walks [78].

Given the small sample of angle swings, additional observations are essential to examine the robustness of these trends. Nevertheless, these trends strongly suggest that the polarization angle rotations may reflect major changes in the jet magnetic field morphology.

### 3. Theoretical Models

As previously mentioned, the long-term polarization signatures appear erratic, which is likely due to instabilities and/or turbulence in the blazar jets. Several works have shown that the observed polarization degree and angle suggest a helical magnetic field structure [82,83]. In some cases, radio observations have shown that blazar activities, including optical polarization variations, are correlated to the emergence of a new radio emission blob [44,62]. However, a detailed theoretical study of such events generally requires a comprehensive modeling of large-scale jet dynamics with particle transport and radiation transfer, which is not mature at present. For the short-term polarization signatures, the frequently observed increasing polarization degree during flares is often interpreted as a shock compressing the initially turbulent magnetic field and accelerating particles [70,71]. Recently, the polarization angle swings have triggered a large number of theoretical studies. They can be generally categorized into geometrical and physical models. In this section, we give a general review of both scenarios.

#### 3.1. Geometrical Models

A bending jet may explain the  $\sim 180^\circ$  polarization angle swing. The idea is that if the jet curvature is confined to a plane inclined to the line of sight within an angle  $\theta_{\text{obs}} < 1/\Gamma_{\text{jet}}$ , where  $\Gamma_{\text{jet}}$  is the jet bulk Lorentz factor, then the curvature alters the projection of the jet magnetic field on the plane of the sky, giving rise to a polarization angle rotation [45]. Such jet configurations are frequently observed in radio observations [84,85]. Due to the change in the Doppler boosting, the bending jet model predicts that the angle rotation should always accompany a blazar flare, which is consistent with current observations. However, the bending jet model can only generate rotation up to  $180^\circ$ . Furthermore, the jet curvature assumed in the model intrinsically links to large-scale jet structure, requiring that all angle rotations in a given source be in the same direction, which contradicts some observations [53,72].

Reference [44] has suggested a spiral motion model where a compact emission blob propagates in a spiral trajectory in a jet pervaded by a helical magnetic field (see Figure 5). The emission blob then lights up the magnetic field structure at its location. Since the magnetic field has a helical shape, this gives rise to the rotating polarization angle. In principle, the amplitude of the rotation can be arbitrary, depending on the helical magnetic field structure and the propagation of the emission blob. The model assumes that the compact emission blob is driven by internal shocks, thus the polarization angle rotation should accompany blazar flares. This model has been successfully applied to several observations [44,45]. However, the direction of the rotation is determined by the helicity of the jet magnetic field, which is unlikely to change in the same blazar. In addition, the propagation of internal shocks in jets should alter the magnetic field structure, which may affect the resulting polarization signatures.

Recently, there have been a couple of new geometric models proposed. Reference [86] has considered the ballistic motion of emission blobs in a jet with a helical magnetic field. Their results have shown that the polarization angle rotations are accompanied by a highly variable polarization degree, which may reach zero during very fast angle rotations. Additionally, the flux is usually at the maximum during fast angle rotations. Reference [87] has proposed a relativistic polarization angle rotation model, where multiple emission blobs in a partially ordered magnetic field may generate angle rotation due to different Doppler boosting. Both models emphasize the effect of the viewing angle, and their results are qualitatively consistent with current observations.

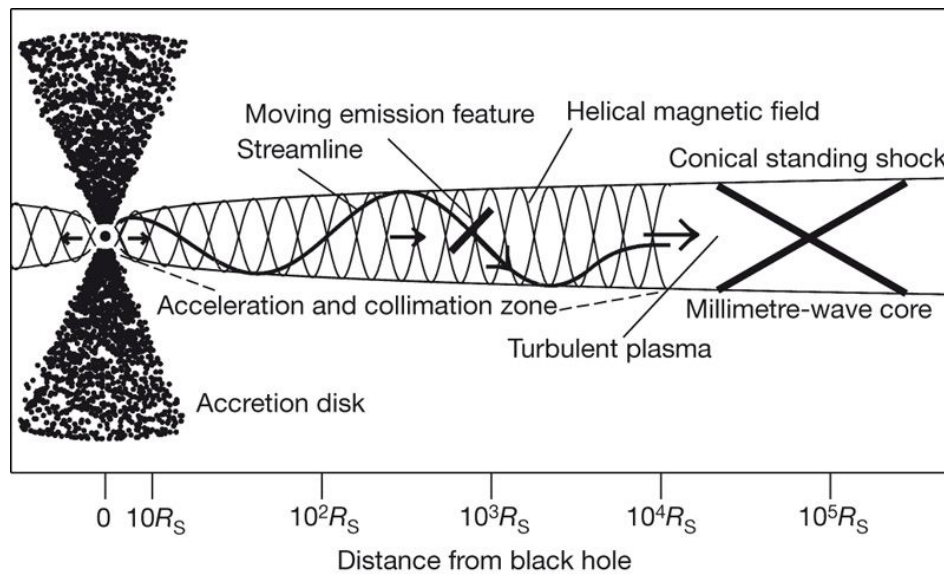


**Figure 5.** A sketch of the spiral motion model. The figure is reproduced from Figure 3 in [44] with permission from Nature.

### 3.2. Physical Models

Given that the observed optical polarization degree is typically below 20%–30%, while the theoretical synchrotron polarization degree in an ordered magnetic field should reach  $\gtrsim 70\%$ , it is very likely that the blazar emission region has a considerable level of turbulence. Reference [71] has put forward a turbulent extreme multi-zone (TEMZ) model to explain the polarization signatures (see Figure 6). The model splits the emission region into a large number of turbulent cells with different magnetic field orientations. The summed synchrotron radiation from these cells can result in a low residual polarization degree with erratic fluctuations in both degree and angle. During active states, shock or magnetic reconnection may inject nonthermal particles and change the magnetic field in some cells, leading to flares and polarization variations. This model has successfully reproduced the typical blazar flares and stochastic polarization signatures. In rare cases, the polarization angle may exhibit large swings. The swings can happen in either direction, with arbitrary amplitude. Due to this stochastic nature, the polarization signatures all appear to be random walks, thus the larger rotations are rarer. Recently, reference [88] has performed particle-in-cell (PIC) simulations of the relaxation of unstable force-free magnetostatic equilibria. The resulting very turbulent magnetic field morphology leads to stochastic polarization signatures, consistent with the predictions of the TEMZ model. However, due to the stochastic nature of this model, the polarization angle swings should be statistically unrelated to the blazar flares, contradicting the RoboPol results [73]. In addition, the RoboPol results do not suggest that all polarization angle swings are random walks [78].

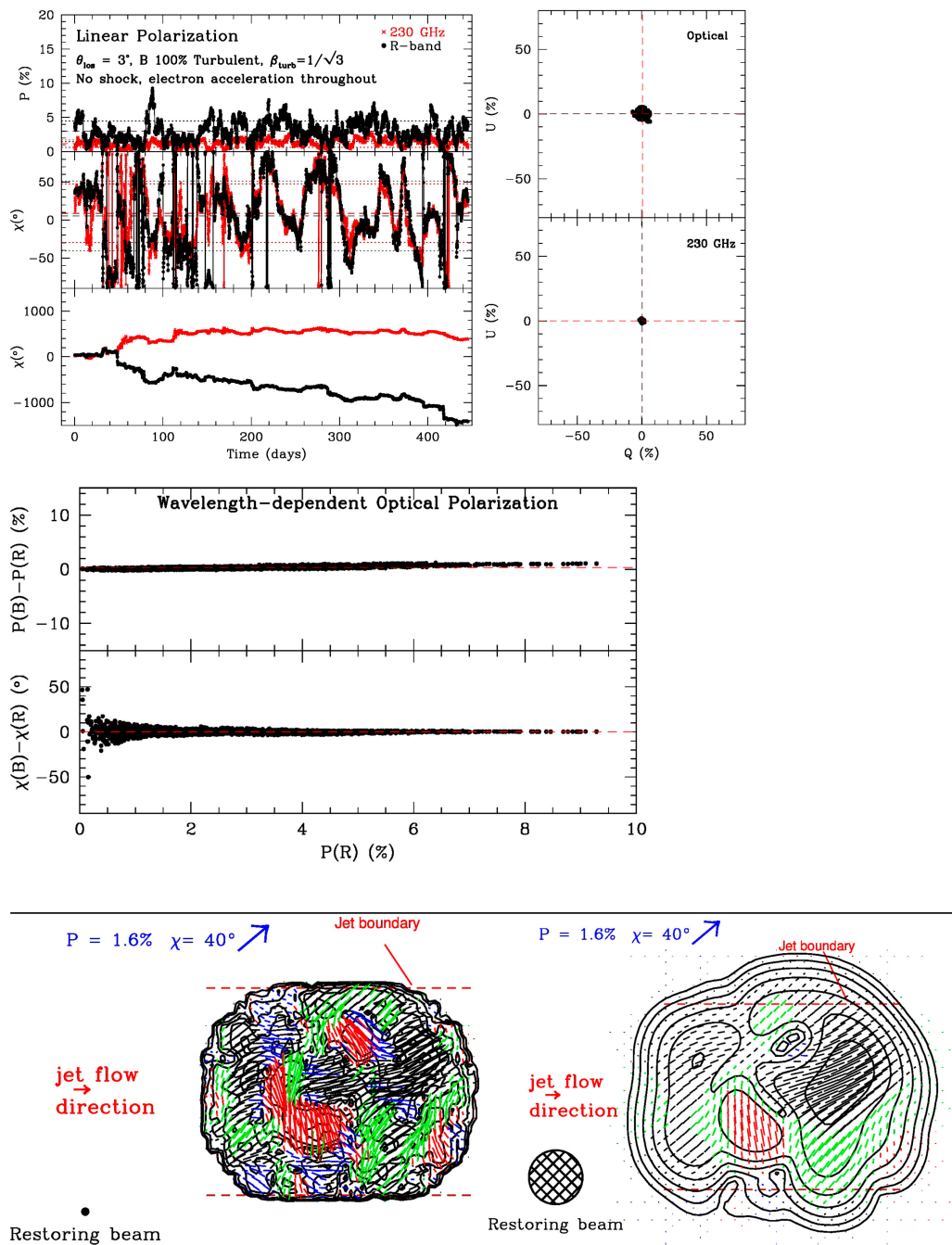


**Figure 6.** Simulated linear polarization behavior over 5000 time-steps generated by the turbulent extreme multi-zone (TEMZ) model for the case of a 100% turbulent magnetic field, no shock, and acceleration of electrons in each of 18,816 cells. Upper left: polarization vs. time; upper right: Stokes Q vs. U scatter plot; middle: color-dependence (B-band minus R-band) of the optical polarization (dashed lines in upper-right and middle plots indicate the mean values); bottom: sample simulated maps of 230 GHz polarized intensity with polarization vectors superposed, convolved with circular Gaussian restoring beams of (left) 2 and (right) 20 microarcseconds FWHM, the former to show the underlying structure, and the latter to approximate the resolution of VLBI at 230 GHz. In the images, the polarization vectors are color-coded according to the 45-degree-wide range in which they fall, for ease of visualization. In this and subsequent figures,  $\beta_{turb}$  is the randomly directed velocity (in units of the speed of light) of the turbulent cells. This figure is reproduced from Figure 2 in [89].

Shock and kink instabilities can efficiently dissipate jet bulk energy to accelerate particles [90–93]. A side effect is that both mechanisms can considerably alter the magnetic field morphology. Reference [94] developed the 3DPol code to study the radiation and polarization signatures of shock and kink instabilities. They have shown that both mechanisms can produce  $\sim 180^\circ$  polarization angle swings along with multi-wavelength emission ([95–97], and see Figure 7). Both mechanisms predict smooth polarization angle rotations on time-scales of days to weeks. Numerical simulations have shown that the angle rotations are in the unit of  $\sim 90^\circ$  for both mechanisms, but neither can go much beyond  $180^\circ$  [97–100]. Another drawback is that the direction of the rotation depends on the helicity of the magnetic field in the emission region, thus the polarization angle prefers to rotate in the same direction in one active epoch. Although this model has successfully reproduced the multi-wavelength radiation and polarization signatures for a couple of events [67,72,96], they cannot account for all of the polarization angle rotations.

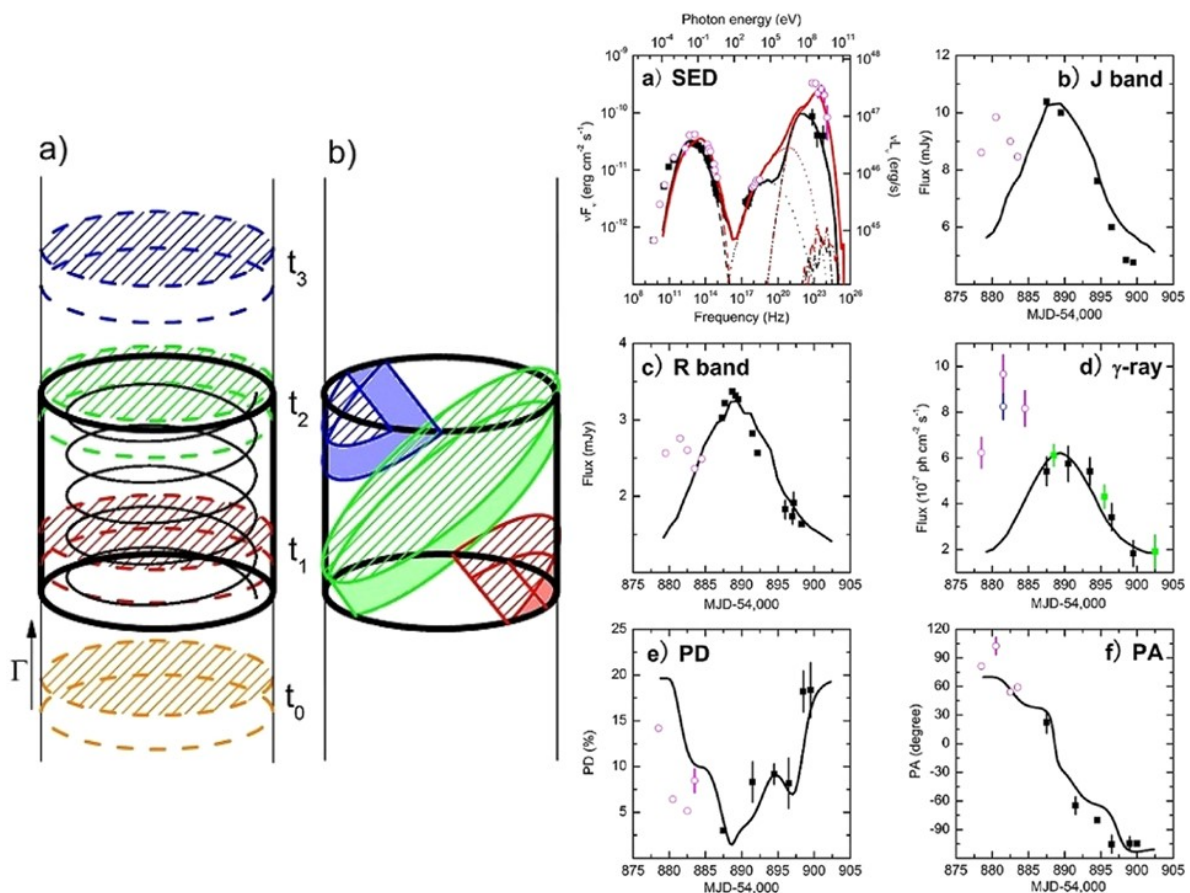


**Figure 7.** (Left): a sketch of the magnetic field geometry and the internal shock model (panel a) and the illustration of light-crossing delay effects (panel b). The different colors in panel a represent the location of the shock at different epochs of the blazar flare. Panel b then shows the apparent location of the shock at equal photon arrival time at the observer. (Right): fittings of spectra, light curves, and polarization signatures of the 3C 279 flaring event [81] based on the model. The figure is reproduced from Figures 4 and 8 in [96] with the permission of the American Astronomical Society (AAS).

Magnetic reconnection can efficiently dissipate magnetic energy to accelerate particles [49,50,101]. In recent years, it has been well studied, both analytically and numerically, that magnetic reconnection can explain the blazar spectra and light curves [88,102–105]. Recently, [106] has combined PIC with polarized radiation transfer simulations to study the polarization signatures during reconnection. Very interestingly, magnetic reconnection can make strong polarization angle swings (see Figure 8). The idea is that the large plasmoids generated in the reconnection layer can merge into each other and

trigger secondary reconnection. This leads to additional particle acceleration where the accelerated particles can stream along the magnetic field lines in the plasmoids, giving rise to polarization angle swings. The rotating angle appears to be in the unit of  $\sim 90^\circ$ , and it can extend well beyond  $180^\circ$ . Additionally, the polarization angle can rotate in either direction. During the swings, the polarization degree usually drops, and there are always flares due to the particle acceleration. This model shows promising features consistent with current observations, but it still needs further examination to test its robustness.

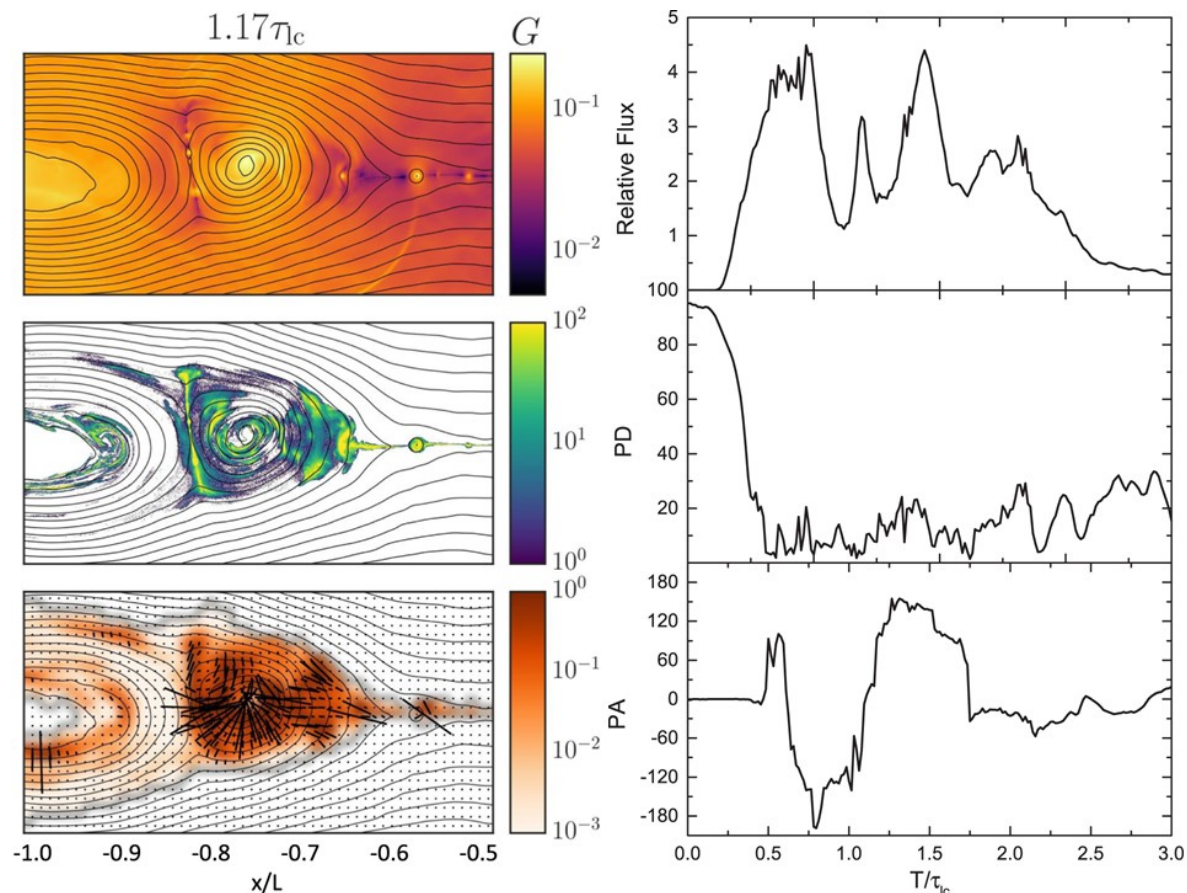


**Figure 8.** (Left): Snapshots of the magnetic field strength (upper row), particle number density (middle row), and the polarized emission map (lower row) of the simulation region. In the lower row, the color indicates the total flux at each zone, while the segments represent the relative polarized flux. (Right): From top to bottom are the relative flux, polarization degree, and angle in the optical band. The figure is reproduced from Figures 2 and 5 in [106] with the permission of the American Astronomical Society (AAS).

#### 4. Future Prospects

The study of AGN jets will become multi-messenger in the next decade. Optical polarimetry will be an important component of multi-messenger studies for two reasons. First, since the correlation of electromagnetic and neutrino signals, and especially their variability, is essential to multi-messenger study, optical polarization variability can provide an additional dimension of observables, providing invaluable constraints for the physical processes in AGN jets. Second, the high-energy polarimetry of AGN jets will become available in the next decade. Synergizing with optical polarimetry, multi-wavelength polarimetry will unveil the high-energy radiation mechanisms and the extreme particle acceleration in AGN jets.

#### 4.1. Polarization Variability

Polarization variability is a very promising research field that can boost our understanding of magnetic field evolution in AGN jets. Recent years of optical polarization monitoring have already made significant breakthroughs in jet dynamics. An important yet not well explored aspect is the statistical trends in the polarization signatures, due to the limited observational data. Continual efforts in polarization monitoring will lead to a better understanding of these trends and the diagnosis of whether the polarization variability is of geometrical or physical origins. Questions to be answered include whether the temporal polarization patterns are different between different optical bands, and when available, X-ray and  $\gamma$ -ray bands; whether polarization angle rotations can be categorized into stochastic and deterministic, and what differences they may have, such as the time scales, polarization degrees, and smoothness; and what makes the blazars with polarization angle rotations different from other blazars. Although some of these questions already have some preliminary answers [58,65,74,80], current results are not fully consistent between different research groups.

In order to better understand the polarization variability, theoretical models need to have a consistent picture of jet dynamics, particle acceleration, and radiation processes. However, the very dynamical and complex nature of AGN jets prevents the use of simple analytical models. Recent first-principle numerical simulations have attempted to consistently combine plasma dynamics and radiation processes to directly compare with observations [88,98,104,105,107], which have shown interesting predictions in polarization variability. With the development of CPU and GPU computing in the next decade, this multi-physics approach will revolutionize our understanding of jet dynamics.

#### 4.2. Multi-Wavelength Polarimetry

High-energy polarimetry will open a new window to study AGN jets. The Imaging X-ray Polarimetry Explorer (IXPE) mission<sup>4</sup> has been selected by NASA for launch in the early 2020s and will explore the X-ray polarization signatures from bright blazars. The All-Sky Medium Energy Gamma-Ray Observatory (AMEGO) mission,<sup>5</sup> if selected, will be capable of detecting polarization from bright blazars in MeV  $\gamma$ -rays.

The X-ray to  $\gamma$ -ray blazar emissions can be polarized [51,108]. Since the optical and high-energy emissions are likely from the same emission region, they should share the same magnetic field morphology. In this situation, [52,107] have shown that the high-energy polarization degree may be detectable with high-energy polarimeters, which can distinguish the leptonic and hadronic models (see Figure 9 left). [109] has studied the temporal behavior of multi-wavelength polarization signatures. Their results have shown that the optical polarization variability can be very different from the high-energy counterparts, which may be used to identify the particle acceleration processes (see Figure 9 (right) for an example). Simultaneous optical and high-energy polarization measurements can examine these predictions.

---

<sup>4</sup> <https://ixpe.msfc.nasa.gov/>.

<sup>5</sup> <https://asd.gsfc.nasa.gov/amego/index.html>.

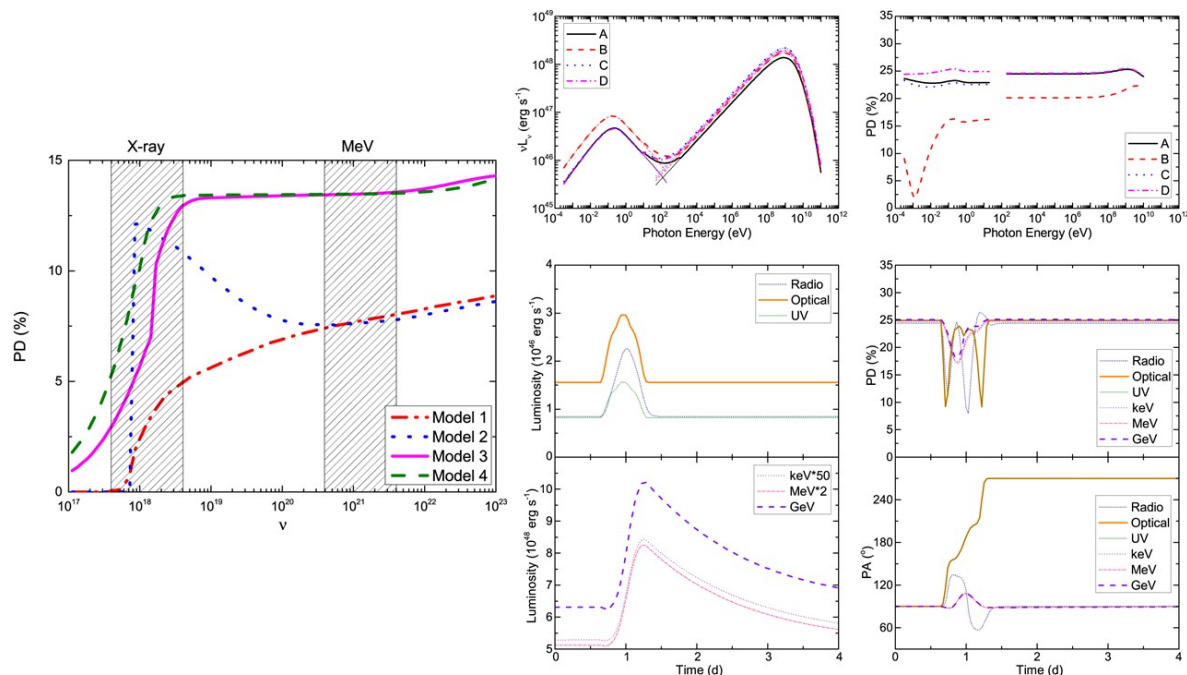


**Figure 9.** Predictions of the spectral and temporal high-energy polarization signatures. **(Left):** The X-ray to  $\gamma$ -ray spectral polarization degree based on the spectral fitting of the TXS 0506+056 observation. The optical polarization degree is taken as 10%. The spectral models 1–4 are the pure leptonic model, leptonic model with a hadronic cascade component, proton synchrotron model with a considerable hadronic cascade component, and proton-synchrotron-dominated model. The shaded regions correspond to the X-ray and MeV  $\gamma$ -ray bands. The figure is reproduced from Figure 2 in [107] with the permission of the American Astronomical Society (AAS). **(Right):** The spectra, light curves, and polarization signatures of the proton-synchrotron-dominated model. The A–D epochs in the upper panels correspond to the spectra and spectral polarization degree before the  $\gamma$ -ray flare, during the rising phase, at the flare peak, and after the flare. This figure is reproduced from Figure 4 in [109] with permission from the American Astronomical Society (AAS).

## 5. Summary

Recent optical polarization monitoring programs have resulted in a rich understanding of polarization variability. In particular, the rare and extreme optical polarization angle swings accompanied by multi-wavelength flares have attracted a lot of attention in the AGN jet community. A number of geometric and physical models have been proposed to explain these phenomena, involving very different jet dynamics and physical processes. Better knowledge of the statistical trends of polarization variability will be essential to distinguish these models in future. Future optical polarimetry will play an essential part in the multi-messenger study of AGN jets. High-energy polarimetry will synergize with optical polarimetry to unveil the radiation and particle acceleration mechanisms in the most violent jet environment.

**Acknowledgments:** H.Z. thanks the anonymous referees for insightful comments. H.Z. thanks Markus Böttcher, Hester Schutte, and Alan Marscher for comments and feedback. H.Z. acknowledges support from Fermi Guest Investigator program Cycle 11, grant No. 80NSSC18K1723 and support from NASA ATP NNX17AG21G and the NSF AST-1816136.

**Conflicts of Interest:** The author declares no conflict of interest.

## References

1. Leahy, J.P.; Williams, A.G. The bridges of classical double radio sources. *Mon. Not. R. Astron. Soc.* **1984**, *210*, 929–951. [[CrossRef](#)]
2. Carilli, C.L.; Barthel, P.D. Cygnus A. *T Astron. Astrophys. Rev.* **1996**, *7*, 1–54. [[CrossRef](#)]
3. MAGIC Collaboration; Albert, J.; Aliu, E.; Anderhub, H.; Antonelli, L.A.; Antoranz, P.; Backes, M.; Baixeras, C.; Barrio, J.A.; Bartko, H.; et al. Very-High-Energy gamma rays from a Distant Quasar: How Transparent Is the Universe? *Science* **2008**, *320*, 1752. [[CrossRef](#)] [[PubMed](#)]
4. Aharonian, F.; Akhperjanian, A.G.; Anton, G.; de Almeida, U.B.; Bazer-Bachi, A.R.; Becherini, Y.; Behera, B.; Benbow, W.; Bernlöhr, K.; Boisson, C.; et al. Discovery of Very High Energy  $\gamma$ -Ray Emission from Centaurus a with H.E.S.S. *Astrophys. J. Lett.* **2009**, *695*, L40–L44. [[CrossRef](#)]
5. Abramowski, A.; Acero, F.; Aharonian, F.; Akhperjanian, A.G.; Anton, G.; Balzer, A.; Barnacka, A.; Barres de Almeida, U.; Becherini, Y.; Becker, J.; et al. The 2010 Very High Energy  $\gamma$ -Ray Flare and 10 Years of Multi-wavelength Observations of M 87. *Astrophys. J.* **2012**, *746*, 151. [[CrossRef](#)]
6. Ahnen, M.L.; Ansoldi, S.; Antonelli, L.A.; Antoranz, P.; Babic, A.; Banerjee, B.; Bangale, P.; Barres de Almeida, U.; Barrio, J.A.; Becerra González, J.; et al. Long-term multi-wavelength variability and correlation study of Markarian 421 from 2007 to 2009. *Astron. Astrophys.* **2016**, *593*, A91. [[CrossRef](#)]
7. Acero, F.; Ackermann, M.; Ajello, M.; Albert, A.; Atwood, W.B.; Axelsson, M.; Baldini, L.; Ballet, J.; Barbiellini, G.; Bastieri, D.; et al. Fermi Large Area Telescope Third Source Catalog. *Astrophys. J. Suppl. Ser.* **2015**, *218*, 23. [[CrossRef](#)]
8. The Fermi-LAT Collaboration. Fermi Large Area Telescope Fourth Source Catalog. *arXiv* **2019**, arXiv:1902.10045.
9. Romero, G.E.; Boettcher, M.; Markoff, S.; Tavecchio, F. Relativistic Jets in Active Galactic Nuclei and Microquasars. *Space Sci. Rev.* **2017**, *207*, 5–61. [[CrossRef](#)]
10. Böttcher, M. Progress in Multi-wavelength and Multi-Messenger Observations of Blazars and Theoretical Challenges. *Galaxies* **2019**, *7*, 20. [[CrossRef](#)]
11. Scarpa, R.; Falomo, R. Are high polarization quasars and BL Lacertae objects really different? A study of the optical spectral properties. *Astron. Astrophys.* **1997**, *325*, 109–123.
12. Lister, M.L.; Aller, M.F.; Aller, H.D.; Hodge, M.A.; Homan, D.C.; Kovalev, Y.Y.; Pushkarev, A.B.; Savolainen, T. MOJAVE. XV. VLBA 15 GHz Total Intensity and Polarization Maps of 437 Parsec-scale AGN Jets from 1996 to 2017. *Astrophys. J. Suppl. Ser.* **2018**, *234*, 12. [[CrossRef](#)]
13. Marscher, A.P.; Gear, W.K. Models for high-frequency radio outbursts in extragalactic sources, with application to the early 1983 millimeter-to-infrared flare of 3C 273. *Astrophys. J.* **1985**, *298*, 114–127. [[CrossRef](#)]
14. Maraschi, L.; Ghisellini, G.; Celotti, A. A jet model for the gamma-ray emitting blazar 3C 279. *Astrophys. J. Lett.* **1992**, *397*, L5–L9. [[CrossRef](#)]
15. Dermer, C.D.; Schlickeiser, R.; Mastichiadis, A. High-energy gamma radiation from extragalactic radio sources. *Astron. Astrophys.* **1992**, *256*, L27–L30.
16. Sikora, M.; Begelman, M.C.; Rees, M.J. Comptonization of diffuse ambient radiation by a relativistic jet: The source of gamma rays from blazars? *Astrophys. J.* **1994**, *421*, 153–162. [[CrossRef](#)]
17. Ghisellini, G.; Madau, P. On the origin of the gamma-ray emission in blazars. *Mon. Not. R. Astron. Soc.* **1996**, *280*, 67–76. [[CrossRef](#)]
18. Böttcher, M.; Reimer, A.; Sweeney, K.; Prakash, A. Leptonic and Hadronic Modeling of Fermi-detected Blazars. *Astrophys. J.* **2013**, *768*, 54. [[CrossRef](#)]
19. Celotti, A.; Ghisellini, G. The power of blazar jets. *Mon. Not. R. Astron. Soc.* **2008**, *385*, 283–300. [[CrossRef](#)]
20. Mannheim, K. The proton blazar. *Astron. Astrophys.* **1993**, *269*, 67–76.
21. Aharonian, F.A. TeV gamma rays from BL Lac objects due to synchrotron radiation of extremely high energy protons. *New Astron.* **2000**, *5*, 377–395. [[CrossRef](#)]
22. Mücke, A.; Protheroe, R.J.; Engel, R.; Rachen, J.P.; Stanev, T. BL Lac objects in the synchrotron proton blazar model. *Astropart. Phys.* **2003**, *18*, 593–613. [[CrossRef](#)]
23. Cerruti, M.; Zech, A.; Boisson, C.; Inoue, S. A hadronic origin for ultra-high-frequency-peaked BL Lac objects. *Mon. Not. R. Astron. Soc.* **2015**, *448*, 910–927. [[CrossRef](#)]
24. Li, H.; Kusunose, M. Temporal and Spectral Variabilities of High-Energy Emission from Blazars Using Synchrotron Self-Compton Models. *Astrophys. J.* **2000**, *536*, 729–741. [[CrossRef](#)]

25. Chen, X.; Fossati, G.; Liang, E.P.; Böttcher, M. Time-dependent simulations of multiwavelength variability of the blazar Mrk 421 with a Monte Carlo multizone code. *Mon. Not. R. Astron. Soc.* **2011**, *416*, 2368–2387. [[CrossRef](#)]
26. Sahu, S.; Oliveros, A.F.O.; Sanabria, J.C. Hadronic-origin orphan TeV flare from 1ES 1959+650. *Phys. Rev. D* **2013**, *87*, 103015. [[CrossRef](#)]
27. Petropoulou, M.; Dimitrakoudis, S.; Padovani, P.; Mastichiadis, A.; Resconi, E. Photohadronic origin of  $\gamma$ -ray BL Lac emission: implications for IceCube neutrinos. *Mon. Not. R. Astron. Soc.* **2015**, *448*, 2412–2429. [[CrossRef](#)]
28. Diltz, C.; Böttcher, M.; Fossati, G. Time Dependent Hadronic Modeling of Flat Spectrum Radio Quasars. *Astrophys. J.* **2015**, *802*, 133. [[CrossRef](#)]
29. IceCube Collaboration; Aartsen, M.G.; Ackermann, M.; Adams, J.; Aguilar, J.A.; Ahlers, M.; Ahrens, M.; Al Samarai, I.; Altmann, D.; Andeen, K.; et al. Multimessenger observations of a flaring blazar coincident with high-energy neutrino IceCube-170922A. *Science* **2018**, *361*, eaat1378. [[CrossRef](#)]
30. IceCube Collaboration; Aartsen, M.G.; Ackermann, M.; Adams, J.; Aguilar, J.A.; Ahlers, M.; Ahrens, M.; Samarai, I.A.; Altmann, D.; Andeen, K.; et al. Neutrino emission from the direction of the blazar TXS 0506+056 prior to the IceCube-170922A alert. *Science* **2018**, *361*, 147–151. [[CrossRef](#)]
31. Ansoldi, S.; Antonelli, L.A.; Arcaro, C.; Baack, D.; Babić, A.; Banerjee, B.; Bangale, P.; Barres de Almeida, U.; Barrio, J.A.; Becerra González, J.; et al. The Blazar TXS 0506+056 Associated with a High-energy Neutrino: Insights into Extragalactic Jets and Cosmic-Ray Acceleration. *Astrophys. J. Lett.* **2018**, *863*, L10. [[CrossRef](#)]
32. Keivani, A.; Murase, K.; Petropoulou, M.; Fox, D.B.; Cenko, S.B.; Chaty, S.; Coleiro, A.; DeLaunay, J.J.; Dimitrakoudis, S.; Evans, P.A.; et al. A Multimessenger Picture of the Flaring Blazar TXS 0506+056: Implications for High-energy Neutrino Emission and Cosmic-Ray Acceleration. *Astrophys. J.* **2018**, *864*, 84. [[CrossRef](#)]
33. Cerruti, M.; Zech, A.; Boisson, C.; Emery, G.; Inoue, S.; Lenain, J.P. Leptohadronic single-zone models for the electromagnetic and neutrino emission of TXS 0506+056. *Mon. Not. R. Astron. Soc.* **2019**, *483*, L12–L16. [[CrossRef](#)]
34. Gao, S.; Fedynitch, A.; Winter, W.; Pohl, M. Modelling the coincident observation of a high-energy neutrino and a bright blazar flare. *Nat. Astron.* **2019**, *3*, 88–92. [[CrossRef](#)]
35. Reimer, A.; Böttcher, M.; Buson, S. Cascading Constraints from Neutrino-emitting Blazars: The Case of TXS 0506+056. *Astrophys. J.* **2019**, *881*, 46. [[CrossRef](#)]
36. Wills, B.J.; Wills, D.; Breger, M.; Antonucci, R.R.J.; Barvainis, R. A Survey for High Optical Polarization in Quasars with Core-dominant Radio Structure: Is There a Beamed Optical Continuum? *Astrophys. J.* **1992**, *398*, 454–475. [[CrossRef](#)]
37. Gabuzda, D.C.; Sitko, M.L. Nearly Simultaneous Very Long Baseline Interferometry and Optical Polarimetry of Blazars. *Astron. J.* **1994**, *107*, 884–991. [[CrossRef](#)]
38. Aller, M.F.; Aller, H.D.; Hughes, P.A.; Latimer, G.E. Centimeter-Wavelength Total Flux and Linear Polarization Properties of Radio-loud BL Lacertae Objects. *Astrophys. J.* **1999**, *512*, 601–622. [[CrossRef](#)]
39. Lister, M.L.; Smith, P.S. Intrinsic Differences in the Inner Jets of High and Low Optically Polarized Radio Quasars. *Astrophys. J.* **2000**, *541*, 66–87. [[CrossRef](#)]
40. Smith, P.S.; Montiel, E.; Rightley, S.; Turner, J.; Schmidt, G.D.; Jannuzi, B.T. Coordinated Fermi/Optical Monitoring of Blazars and the Great 2009 September Gamma-ray Flare of 3C 454.3. *arXiv* **2009**, arXiv:0912.3621
41. D’Ammando, F.; Raiteri, C.M.; Villata, M.; Romano, P.; Pucella, G.; Krimm, H.A.; Covino, S.; Orienti, M.; Giovannini, G.; Vercellone, S.; et al. AGILE detection of extreme  $\gamma$ -ray activity from the blazar PKS 1510-089 during March 2009. Multifrequency analysis. *Astron. Astrophys.* **2011**, *529*, A145. [[CrossRef](#)]
42. Ikejiri, Y.; Uemura, M.; Sasada, M.; Ito, R.; Yamanaka, M.; Sakimoto, K.; Arai, A.; Fukazawa, Y.; Ohsugi, T.; Kawabata, K.S.; et al. Photopolarimetric Monitoring of Blazars in the Optical and Near-Infrared Bands with the Kanata Telescope. I. Correlations between Flux, Color, and Polarization. *Publ. Astron. Soc. Jpn.* **2011**, *63*, 639–675. [[CrossRef](#)]
43. Aleksić, J.; Ansoldi, S.; Antonelli, L.A.; Antoranz, P.; Babic, A.; Bangale, P.; Barres de Almeida, U.; Barrio, J.A.; Becerra González, J.; Bednarek, W.; et al. MAGIC gamma-ray and multi-frequency observations of flat spectrum radio quasar PKS 1510-089 in early 2012. *Astron. Astrophys.* **2014**, *569*, A46. [[CrossRef](#)]

44. Marscher, A.P.; Jorstad, S.G.; D’Arcangelo, F.D.; Smith, P.S.; Williams, G.G.; Larionov, V.M.; Oh, H.; Olmstead, A.R.; Aller, M.F.; Aller, H.D.; et al. The inner jet of an active galactic nucleus as revealed by a radio-to- $\gamma$ -ray outburst. *Nature* **2008**, *452*, 966–969. [[CrossRef](#)] [[PubMed](#)]
45. Larionov, V.M.; Jorstad, S.G.; Marscher, A.P.; Morozova, D.A.; Blinov, D.A.; Hagen-Thorn, V.A.; Konstantinova, T.S.; Kopatskaya, E.N.; Larionova, L.V.; Larionova, E.G.; et al. The Outburst of the Blazar S5 0716+71 in 2011 October: Shock in a Helical Jet. *Astrophys. J.* **2013**, *768*, 40. [[CrossRef](#)]
46. Blinov, D.; Pavlidou, V.; Papadakis, I.; Kiehlmann, S.; Panopoulou, G.; Liodakis, I.; King, O.G.; Angelakis, E.; Baloković, M.; Das, H.; et al. RoboPol: First season rotations of optical polarization plane in blazars. *Mon. Not. R. Astron. Soc.* **2015**, *453*, 1669–1683. [[CrossRef](#)]
47. Summerlin, E.J.; Baring, M.G. Diffusive Acceleration of Particles at Oblique, Relativistic, Magnetohydrodynamic Shocks. *Astrophys. J.* **2012**, *745*, 63. [[CrossRef](#)]
48. O’Neill, S.M.; Beckwith, K.; Begelman, M.C. Local simulations of instabilities in relativistic jets—I. Morphology and energetics of the current-driven instability. *Mon. Not. R. Astron. Soc.* **2012**, *422*, 1436–1452. [[CrossRef](#)]
49. Sironi, L.; Spitkovsky, A. Relativistic Reconnection: An Efficient Source of Non-thermal Particles. *Astrophys. J. Lett.* **2014**, *783*, L21. [[CrossRef](#)]
50. Guo, F.; Li, H.; Daughton, W.; Liu, Y.H. Formation of Hard Power Laws in the Energetic Particle Spectra Resulting from Relativistic Magnetic Reconnection. *Phys. Rev. Lett.* **2014**, *113*, 155005. [[CrossRef](#)]
51. Zhang, H.; Böttcher, M. X-Ray and Gamma-Ray Polarization in Leptonic and Hadronic Jet Models of Blazars. *Astrophys. J.* **2013**, *774*, 18. [[CrossRef](#)]
52. Paliya, V.S.; Zhang, H.; Böttcher, M.; Ajello, M.; Domínguez, A.; Joshi, M.; Hartmann, D.; Stalin, C.S. Leptonic and Hadronic Modeling of Fermi-LAT Hard Spectrum Quasars and Predictions for High-energy Polarization. *Astrophys. J.* **2018**, *863*, 98. [[CrossRef](#)]
53. Morozova, D.A.; Larionov, V.M.; Troitsky, I.S.; Jorstad, S.G.; Marscher, A.P.; Gómez, J.L.; Blinov, D.A.; Efimova, N.V.; Hagen-Thorn, V.A.; Hagen-Thorn, E.I.; et al. The Outburst of the Blazar S4 0954+658 in 2011 March–April. *Astron. J.* **2014**, *148*, 42. [[CrossRef](#)]
54. Smith, P.S. Extremely High Optical Polarization Observed in the Blazar PKS1502+106. *Astron. Telegr.* **2017**, *11047*, 1.
55. Hutsemékers, D.; Borguet, B.; Sluse, D.; Cabanac, R.; Lamy, H. Optical circular polarization in quasars. *Astron. Astrophys.* **2010**, *520*, L7. [[CrossRef](#)]
56. Itoh, R.; Fukazawa, Y.; Tanaka, Y.T.; Abe, Y.; Akitaya, H.; Arai, A.; Hayashi, M.; Hori, T.; Isogai, M.; Izumiura, H.; et al. Dense Optical and Near-infrared Monitoring of CTA 102 during High State in 2012 with OISTER: Detection of Intra-night “Orphan Polarized Flux Flare”. *Astrophys. J. Lett.* **2013**, *768*, L24. [[CrossRef](#)]
57. Marscher, A.P.; Jorstad, S.G.; Larionov, V.M.; Aller, M.F.; Aller, H.D.; Lähteenmäki, A.; Agudo, I.; Smith, P.S.; Gurwell, M.; Hagen-Thorn, V.A.; et al. Probing the Inner Jet of the Quasar PKS 1510-089 with Multi-Waveband Monitoring During Strong Gamma-Ray Activity. *Astrophys. J. Lett.* **2010**, *710*, L126–L131. [[CrossRef](#)]
58. Itoh, R.; Nalewajko, K.; Fukazawa, Y.; Uemura, M.; Tanaka, Y.T.; Kawabata, K.S.; Madejski, G.M.; Schinzel, F.K.; Kanda, Y.; Shiki, K.; et al. Systematic Study of Gamma-ray-bright Blazars with Optical Polarization and Gamma-Ray Variability. *Astrophys. J.* **2016**, *833*, 77. [[CrossRef](#)]
59. Pekeur, N.W.; Taylor, A.R.; Potter, S.B.; Kraan-Korteweg, R.C. Evidence for quasi-periodic oscillations in the optical polarization of the blazar PKS 2155-304. *Mon. Not. R. Astron. Soc.* **2016**, *462*, L80–L83. [[CrossRef](#)]
60. Böttcher, M.; van Soelen, B.; Britto, R.; Buckley, D.; Marais, J.; Schutte, H. SALT Spectropolarimetry and Self-Consistent SED and Polarization Modeling of Blazars. *Galaxies* **2017**, *5*, 52. [[CrossRef](#)]
61. Aliu, E.; Archambault, S.; Archer, A.; Arlen, T.; Aune, T.; Barnacka, A.; Behera, B.; Beilicke, M.; Benbow, W.; Berger, K.; et al. Very high energy outburst of Markarian 501 in May 2009. *Astron. Astrophys.* **2016**, *594*, A76. [[CrossRef](#)]
62. Jorstad, S.G.; Marscher, A.P.; Smith, P.S.; Larionov, V.M.; Agudo, I.; Gurwell, M.; Wehrle, A.E.; Lähteenmäki, A.; Nikolashvili, M.G.; Schmidt, G.D.; et al. A Tight Connection between Gamma-Ray Outbursts and Parsec-scale Jet Activity in the Quasar 3C 454.3. *Astrophys. J.* **2013**, *773*, 147. [[CrossRef](#)]
63. Rani, B.; Jorstad, S.G.; Marscher, A.P.; Agudo, I.; Sokolovsky, K.V.; Larionov, V.M.; Smith, P.; Mosunova, D.A.; Borman, G.A.; Grishina, T.S.; et al. Exploring the Connection between Parsec-scale Jet Activity and Broadband Outbursts in 3C 279. *Astrophys. J.* **2018**, *858*, 80. [[CrossRef](#)]

64. Patiño-Álvarez, V.M.; Fernandes, S.; Chavushyan, V.; López-Rodríguez, E.; León-Tavares, J.; Schlegel, E.M.; Carrasco, L.; Valdés, J.; Carramiñana, A. Multiwavelength photometric and spectropolarimetric analysis of the FSRQ 3C 279. *Mon. Not. R. Astron. Soc.* **2018**, *479*, 2037–2064. [[CrossRef](#)]
65. Jermak, H.; Steele, I.A.; Lindfors, E.; Hovatta, T.; Nilsson, K.; Lamb, G.P.; Mundell, C.; Barres de Almeida, U.; Berdyugin, A.; Kadenius, V.; et al. The RINGO2 and DIPOL optical polarization catalogue of blazars. *Mon. Not. R. Astron. Soc.* **2016**, *462*, 4267–4299. [[CrossRef](#)]
66. Andruchow, I.; Cellone, S.A.; Romero, G.E.; Dominici, T.P.; Abraham, Z. Microvariability in the optical polarization of 3C 279. *Astron. Astrophys.* **2003**, *409*, 857–865. [[CrossRef](#)]
67. Covino, S.; Baglio, M.C.; Foschini, L.; Sandrinelli, A.; Tavecchio, F.; Treves, A.; Zhang, H.; Barres de Almeida, U.; Bonnoli, G.; Böttcher, M.; et al. Short timescale photometric and polarimetric behavior of two BL Lacertae type objects. *Astron. Astrophys.* **2015**, *578*, A68. [[CrossRef](#)]
68. Cellone, S.A.; Romero, G.E.; Combi, J.A.; Martí, J. Extreme photopolarimetric behaviour of the blazar AO0235+164. *Mon. Not. R. Astron. Soc.* **2007**, *381*, L60–L64. [[CrossRef](#)]
69. Hagen-Thorn, V.A.; Larionov, V.M.; Jorstad, S.G.; Arkharov, A.A.; Hagen-Thorn, E.I.; Efimova, N.V.; Larionova, L.V.; Marscher, A.P. The Outburst of the Blazar AO 0235+164 in 2006 December: Shock-in-Jet Interpretation. *Astrophys. J.* **2008**, *672*, 40–47. [[CrossRef](#)]
70. Laing, R.A. A model for the magnetic-field structure in extended radio sources. *Mon. Not. R. Astron. Soc.* **1980**, *193*, 439–449. [[CrossRef](#)]
71. Marscher, A.P. Turbulent, Extreme Multi-zone Model for Simulating Flux and Polarization Variability in Blazars. *Astrophys. J.* **2014**, *780*, 87. [[CrossRef](#)]
72. Chandra, S.; Zhang, H.; Kushwaha, P.; Singh, K.P.; Böttcher, M.; Kaur, N.; Baliyan, K.S. Multi-wavelength Study of Flaring Activity in BL Lac Object S5 0716+714 during the 2015 Outburst. *Astrophys. J.* **2015**, *809*, 130. [[CrossRef](#)]
73. Blinov, D.; Pavlidou, V.; Papadakis, I.; Kiehlmann, S.; Lioudakis, I.; Panopoulou, G.V.; Angelakis, E.; Baloković, M.; Hovatta, T.; King, O.G.; et al. RoboPol: Connection between optical polarization plane rotations and gamma-ray flares in blazars. *Mon. Not. R. Astron. Soc.* **2018**, *474*, 1296–1306. [[CrossRef](#)]
74. Angelakis, E.; Hovatta, T.; Blinov, D.; Pavlidou, V.; Kiehlmann, S.; Myserlis, I.; Böttcher, M.; Mao, P.; Panopoulou, G.V.; Lioudakis, I.; et al. RoboPol: The optical polarization of gamma-ray-loud and gamma-ray-quiet blazars. *Mon. Not. R. Astron. Soc.* **2016**, *463*, 3365–3380. [[CrossRef](#)]
75. Hovatta, T.; Lindfors, E.; Blinov, D.; Pavlidou, V.; Nilsson, K.; Kiehlmann, S.; Angelakis, E.; Fallah Ramazani, V.; Lioudakis, I.; Myserlis, I.; et al. Optical polarization of high-energy BL Lacertae objects. *Astron. Astrophys.* **2016**, *596*, A78. [[CrossRef](#)]
76. Jannuzi, B.T.; Smith, P.S.; Elston, R. The Optical Polarization Properties of X-ray—Selected BL Lacertae Objects. *Astrophys. J.* **1994**, *428*, 130. [[CrossRef](#)]
77. Smith, P.S.; Williams, G.G.; Schmidt, G.D.; Diamond-Stanic, A.M.; Means, D.L. Highly Polarized Optically Selected BL Lacertae Objects. *Astrophys. J.* **2007**, *663*, 118–124. [[CrossRef](#)]
78. Kiehlmann, S.; Blinov, D.; Pearson, T.J.; Lioudakis, I. Optical EVPA rotations in blazars: Testing a stochastic variability model with RoboPol data. *Mon. Not. R. Astron. Soc.* **2017**, *472*, 3589–3604. [[CrossRef](#)]
79. Fossati, G.; Maraschi, L.; Celotti, A.; Comastri, A.; Ghisellini, G. A unifying view of the spectral energy distributions of blazars. *Mon. Not. R. Astron. Soc.* **1998**, *299*, 433–448. [[CrossRef](#)]
80. Blinov, D.; Pavlidou, V.; Papadakis, I.E.; Hovatta, T.; Pearson, T.J.; Lioudakis, I.; Panopoulou, G.V.; Angelakis, E.; Baloković, M.; Das, H.; et al. RoboPol: Optical polarization-plane rotations and flaring activity in blazars. *Mon. Not. R. Astron. Soc.* **2016**, *457*, 2252–2262. [[CrossRef](#)]
81. Abdo, A.A.; Ackermann, M.; Ajello, M.; Axelsson, M.; Baldini, L.; Ballet, J.; Barbiellini, G.; Bastieri, D.; Baughman, B.M.; Bechtol, K.; et al. A change in the optical polarization associated with a  $\gamma$ -ray flare in the blazar 3C279. *Nature* **2010**, *463*, 919–923. [[CrossRef](#)]
82. Lyutikov, M.; Pariev, V.I.; Gabuzda, D.C. Polarization and structure of relativistic parsec-scale AGN jets. *Mon. Not. R. Astron. Soc.* **2005**, *360*, 869–891. [[CrossRef](#)]
83. Pushkarev, A.B.; Gabuzda, D.C.; Vetukhnovskaya, Y.N.; Yakimov, V.E. Spine-sheath polarization structures in four active galactic nuclei jets. *Mon. Not. R. Astron. Soc.* **2005**, *356*, 859–871. [[CrossRef](#)]
84. Homan, D.C.; Wardle, J.F.C.; Cheung, C.C.; Roberts, D.H.; Attridge, J.M. PKS 1510-089: A Head-on View of a Relativistic Jet. *Astrophys. J.* **2002**, *580*, 742–748. [[CrossRef](#)]

85. Lister, M.L.; Aller, M.F.; Aller, H.D.; Homan, D.C.; Kellermann, K.I.; Kovalev, Y.Y.; Pushkarev, A.B.; Richards, J.L.; Ros, E.; Savolainen, T. MOJAVE. X. Parsec-scale Jet Orientation Variations and Superluminal Motion in Active Galactic Nuclei. *Astron. J.* **2013**, *146*, 120. [[CrossRef](#)]
86. Lyutikov, M.; Kravchenko, E.V. Polarization swings in blazars. *Mon. Not. R. Astron. Soc.* **2017**, *467*, 3876–3886. [[CrossRef](#)]
87. Peirson, A.L.; Romani, R.W. The Polarization Behavior of Relativistic Synchrotron Jets. *Astrophys. J.* **2018**, *864*, 140. [[CrossRef](#)]
88. Yuan, Y.; Nalewajko, K.; Zrake, J.; East, W.E.; Blandford, R.D. Kinetic Study of Radiation-reaction-limited Particle Acceleration During the Relaxation of Unstable Force-free Equilibria. *Astrophys. J.* **2016**, *828*, 92. [[CrossRef](#)]
89. Marscher, A.; Jorstad, S.; Williamson, K. Modeling the Time-Dependent Polarization of Blazars. *Galaxies* **2017**, *5*, 63. [[CrossRef](#)]
90. Achterberg, A.; Gallant, Y.A.; Kirk, J.G.; Guthmann, A.W. Particle acceleration by ultrarelativistic shocks: Theory and simulations. *Mon. Not. R. Astron. Soc.* **2001**, *328*, 393–408. [[CrossRef](#)]
91. Spitkovsky, A. Particle Acceleration in Relativistic Collisionless Shocks: Fermi Process at Last? *Astrophys. J. Lett.* **2008**, *682*, L5. [[CrossRef](#)]
92. Mizuno, Y.; Lyubarsky, Y.; Nishikawa, K.I.; Hardee, P.E. Three-Dimensional Relativistic Magnetohydrodynamic Simulations of Current-Driven Instability. I. Instability of a Static Column. *Astrophys. J.* **2009**, *700*, 684–693. [[CrossRef](#)]
93. Alves, E.P.; Zrake, J.; Fiuza, F. Efficient Nonthermal Particle Acceleration by the Kink Instability in Relativistic Jets. *PRL* **2018**, *121*, 245101. [[CrossRef](#)] [[PubMed](#)]
94. Zhang, H.; Chen, X.; Böttcher, M. Synchrotron Polarization in Blazars. *Astrophys. J.* **2014**, *789*, 66. [[CrossRef](#)]
95. Chen, X.; Chatterjee, R.; Zhang, H.; Pohl, M.; Fossati, G.; Böttcher, M.; Baily, C.D.; Bonning, E.W.; Buxton, M.; Coppi, P.; et al. Magnetic field amplification and flat spectrum radio quasars. *Mon. Not. R. Astron. Soc.* **2014**, *441*, 2188–2199. [[CrossRef](#)]
96. Zhang, H.; Chen, X.; Böttcher, M.; Guo, F.; Li, H. Polarization Swings Reveal Magnetic Energy Dissipation in Blazars. *Astrophys. J.* **2015**, *804*, 58. [[CrossRef](#)]
97. Zhang, H.; Li, H.; Guo, F.; Taylor, G. Polarization Signatures of Kink Instabilities in the Blazar Emission Region from Relativistic Magnetohydrodynamic Simulations. *Astrophys. J.* **2017**, *835*, 125. [[CrossRef](#)]
98. Zhang, H.; Deng, W.; Li, H.; Böttcher, M. Polarization Signatures of Relativistic Magnetohydrodynamic Shocks in the Blazar Emission Region. I. Force-free Helical Magnetic Fields. *Astrophys. J.* **2016**, *817*, 63. [[CrossRef](#)]
99. Deng, W.; Zhang, H.; Zhang, B.; Li, H. Collision-induced Magnetic Reconnection and a Unified Interpretation of Polarization Properties of GRBs and Blazars. *Astrophys. J. Lett.* **2016**, *821*, L12. [[CrossRef](#)]
100. Nalewajko, K. A Model of Polarisation Rotations in Blazars from Kink Instabilities in Relativistic Jets. *Galaxies* **2017**, *5*, 64. [[CrossRef](#)]
101. Giannios, D.; Uzdensky, D.A.; Begelman, M.C. Fast TeV variability in blazars: Jets in a jet. *Mon. Not. R. Astron. Soc.* **2009**, *395*, L29–L33. [[CrossRef](#)]
102. Sironi, L.; Petropoulou, M.; Giannios, D. Relativistic jets shine through shocks or magnetic reconnection? *Mon. Not. R. Astron. Soc.* **2015**, *450*, 183–191. [[CrossRef](#)]
103. Guo, F.; Li, X.; Li, H.; Daughton, W.; Zhang, B.; Lloyd-Ronning, N.; Liu, Y.H.; Zhang, H.; Deng, W. Efficient Production of High-energy Nonthermal Particles during Magnetic Reconnection in a Magnetically Dominated Ion-Electron Plasma. *Astrophys. J. Lett.* **2016**, *818*, L9. [[CrossRef](#)]
104. Petropoulou, M.; Giannios, D.; Sironi, L. Blazar flares powered by plasmoids in relativistic reconnection. *Mon. Not. R. Astron. Soc.* **2016**, *462*, 3325–3343. [[CrossRef](#)]
105. Christie, I.M.; Petropoulou, M.; Sironi, L.; Giannios, D. Radiative signatures of plasmoid-dominated reconnection in blazar jets. *Mon. Not. R. Astron. Soc.* **2019**, *482*, 65–82. [[CrossRef](#)]
106. Zhang, H.; Li, X.; Guo, F.; Giannios, D. Large-amplitude Blazar Polarization Angle Swing as a Signature of Magnetic Reconnection. *Astrophys. J. Lett.* **2018**, *862*, L25. [[CrossRef](#)]
107. Zhang, H.; Fang, K.; Li, H.; Giannios, D.; Böttcher, M.; Buson, S. Probing the Emission Mechanism and Magnetic Field of Neutrino Blazars with Multiwavelength Polarization Signatures. *Astrophys. J.* **2019**, *876*, 109. [[CrossRef](#)]

108. Krawczynski, H. The Polarization Properties of Inverse Compton Emission and Implications for Blazar Observations with the GEMS X-Ray Polarimeter. *Astrophys. J.* **2012**, *744*, 30. [[CrossRef](#)]
109. Zhang, H.; Diltz, C.; Böttcher, M. Radiation and Polarization Signatures of the 3D Multizone Time-dependent Hadronic Blazar Model. *Astrophys. J.* **2016**, *829*, 69. [[CrossRef](#)]



© 2019 by the authors. Licensee MDPI, Basel, Switzerland. This article is an open access article distributed under the terms and conditions of the Creative Commons Attribution (CC BY) license (<http://creativecommons.org/licenses/by/4.0/>).